ISSN 1674-1056
http://cpb.iphy.ac.cn
http://iopscience.iop.org/cpb
中国物理 B
Chinese Physics
中国物理 Chinese Physics B

Pre- and post-selected measurements with coupling-strength-dependent modulation

Zhaoxue Li(李兆雪), Jiangdong Qiu(邱疆冬), Linguo Xie(谢林果), Lan Luo(罗兰), Xiong Liu(刘雄), Zhiyou Zhang(张志友), Changliang Ren(任昌亮), JingLei Du(杜惊雷)

Citation: Chin. Phys. B . 2019, 28(3): 030602. **doi:** 10.1088/1674-1056/28/3/030602
Journal homepage: http://cpb.iphy.ac.cn; http://iopscience.iop.org/cpb

What follows is a list of articles you may be interested in

Quantum parameter estimation in a spin-boson dephasing quantum system by periodical projective measurements

Le Yang(杨乐), Hong-Yi Dai(戴宏毅), Ming Zhang(张明)

Chin. Phys. B . 2018, 27(4): 040601. **doi:** 10.1088/1674-1056/27/4/040601

Optimal quantum parameter estimation of two-qutrit Heisenberg *XY* chain under decoherence

Hong-ying Yang(杨洪应), Qiang Zheng(郑强), Qi-jun Zhi(支启军)

Chin. Phys. B . 2017, 26(1): 010601. **doi:** 10.1088/1674-1056/26/1/010601

Phase sensitivity of two nonlinear interferometers with inputting entangled coherent states

Chao-Ping Wei(魏朝平), Xiao-Yu Hu(胡小玉), Ya-Fei Yu(於亚飞), Zhi-Ming Zhang(张智明)

Chin. Phys. B . 2016, 25(4): 040601. **doi:** 10.1088/1674-1056/25/4/040601

Progress on accurate measurement of the Planck constant: Watt balance and counting atoms

Li Shi-Song, Zhang Zhong-Hua, Zhao Wei, Li Zheng-Kun, Huang Song-Ling

Chin. Phys. B . 2015, 24(1): 010601. **doi:** 10.1088/1674-1056/24/1/010601

Enhancing the precision of phase estimation by weak measurement and quantum measurement reversal

He Zhi, Yao Chun-Mei

Chin. Phys. B . 2014, 23(11): 110601. **doi:** 10.1088/1674-1056/23/11/110601

Pre- and post-selected measurements with coupling-strength-dependent modulation*

Zhaoxue Li(李兆雪)[1], Jiangdong Qiu(邱疆冬)[1], Linguo Xie(谢林果)[1], Lan Luo(罗兰)[1], Xiong Liu(刘雄)[1], Zhiyou Zhang(张志友)[1,2,†], Changliang Ren(任昌亮)[3,‡], and JingLei Du(杜惊雷)[1,2]

[1] *College of Physical Science and Technology, Sichuan University, Chengdu* 610064, *China*

[2] *Key Laboratory of High Energy Density Physics and Technology of Ministry of Education, Sichuan University, Chengdu* 610064, *China*

[3] *Chongqing Institute of Green and Intelligent Technology, Chinese Academy of Sciences, Chongqing* 400714, *China*

(Received 7 September 2018; revised manuscript received 24 December 2018; published online 26 February 2019)

Pre- and post-selected (PPS) measurement, especially the weak PPS measurement, has been proved to be a useful tool for measuring extremely tiny physical parameters. However, it is difficult to retain both the attainable highest measurement sensitivity and precision with the increase of the parameter to be measured. Here, a modulated PPS measurement scheme based on coupling-strength-dependent modulation is presented with the highest sensitivity and precision retained for an arbitrary coupling strength. This idea is demonstrated by comparing the modulated PPS measurement scheme with the standard PPS measurement scheme in the case of unbalanced input meter. By using the Fisher information metric, we derive the optimal pre- and post-selected states, as well as the optimal coupling-strength-dependent modulation without any restriction on the coupling strength. We also give the specific strategy of performing the modulated PPS measurement scheme, which may promote practical application of this scheme in precision metrology.

Keywords: modulated pre- and post-selected measurements, Fisher information metric, unbalanced input meter

PACS: 06.20.–f, 42.50.Dv, 42.50.Xa **DOI:** 10.1088/1674-1056/28/3/030602

1. Introduction

Pre- and post-selected (PPS) measurement, which was first proposed by Aharonov, Bergmann, and Lebowitz (ABL), is of fundamental significance in quantum measurement.[1] PPS measurement is performed on a sub-ensemble of a system with chosen pre- and post-selected states. The coupling strength between the system and the meter can be measured with a subsequent projective measurement of the output meter. A typical extension of PPS measurement is the weak PPS measurement (i.e., the so-called weak measurement), which requires an extremely weak coupling strength.[2–4] Weak measurement has attracted much attention due to the striking amplification effect on some ultra-small physical parameters with an amplification factor of the weak value[5–19]

$$A_{\rm w}=\frac{\langle\psi_{\rm f}|\hat{A}|\psi_{\rm i}\rangle}{\langle\psi_{\rm f}|\psi_{\rm i}\rangle}, \tag{1}$$

where $\hat{A}$ denotes the observable of the system, and $|\psi_{\rm i}\rangle$ and $|\psi_{\rm f}\rangle$ denote the pre- and post-selected states of the system, respectively. In principle, the weak value can be very large even to far exceed the eigenvalue spectra of $\hat{A}$ when $\langle\psi_{\rm f}|\psi_{\rm i}\rangle\to 0$.[2,20] Consider a physical parameter serving as the coupling strength γ in an interaction Hamilton $\hat{H}=\gamma\hat{A}\otimes\hat{F}$ with F being the input meter variable, the meter state after post-selection on the system can be written as

$$\begin{aligned}\langle\psi_{\rm f}|\Psi\rangle &= \langle\psi_{\rm f}|\exp(-{\rm i}\gamma\hat{A}\otimes\hat{F})|\psi_{\rm i}\rangle|\Phi_{\rm i}\rangle\\ &\simeq \langle\psi_{\rm f}|1-{\rm i}\gamma\hat{A}\otimes\hat{F}|\psi_{\rm i}\rangle|\Phi_{\rm i}\rangle\\ &\simeq \langle\psi_{\rm f}|\exp(-{\rm i}\gamma A_{\rm w}\hat{F})|\psi_{\rm i}\rangle|\Phi_{\rm i}\rangle,\end{aligned} \tag{2}$$

where $|\Phi_{\rm i}\rangle$ represents the initial meter state. Traditionally, the meter wave function is taken as the real Gaussian with a standard deviation of ΔF. The first inequality in Eq. (2) results from a weak coupling strength satisfying $|\gamma|\Delta F\ll 1$, and the second inequality requires a weaker coupling satisfying $|\gamma A_{\rm w}|\Delta F\ll 1$.[4,21–23] Consider a meter with coinciding input and output variables (i.e., $R=F$), one can always extract the coupling strength from the average pointer deflection in the linear-response regime

$$\Delta\langle F\rangle\simeq 2\gamma(\Delta F)^2\,{\rm Im}(A_{\rm w}), \tag{3}$$

i.e., linearly weak-value amplification (WVA) with high-precision. However, such linear WVA is valid only for measuring extremely small parameters in the case of balanced input meter ($\bar{F}=0$), such as the detection in position space.[11,24]

*Project supported by the National Natural Science Foundation of China (Grant Nos. 11674234 and 11605205), the Fundamental Research Funds for the Central Universities, China (Grant No. 2012017yjsy143), the National Key Research and Development Program of China (Grant No. 2017YFA0305200), the Youth Innovation Promotion Association of Chinese Academy of Sciences (CAS) (Grant No. 2015317), the Natural Science Foundation of Chongqing, China (Grant Nos. cstc2015jcyjA00021 and cstc2018jcyjAX0656), the Entrepreneurship and Innovation Support Program for Chongqing Overseas Returnees, China (Grant No. cx017134), the Fund of CAS Key Laboratory of Microscale Magnetic Resonance, China, and the Fund of CAS Key Laboratory of Quantum Information, China.

†Corresponding author. E-mail: zhangzhiyou@scu.edu.cn

‡Corresponding author. E-mail: renchangliang@cigit.ac.cn

© 2019 Chinese Physical Society and IOP Publishing Ltd

In fact, there exist many scenarios involving an unbalanced input meter which requires a nonzero expected value for the input meter variable ($\bar{F} \neq 0$), such as the detection in frequency space.[10,25] For the cases of balanced and unbalanced input meters, it is difficult to retain both the attainable highest measurement sensitivity and precision with the increase of the coupling strength, even within the weak coupling limit. To address this problem, Zhang *et al*. recently introduced a bias phase approximating to the post-selected angle, which has the potential to retain the measurement sensitivity only for extremely weak coupling strength.[26] More recently, Li *et al*. proposed an adaptive WVA scheme to retain the ultra-high precision, in which the coupling strength can be relaxed to $|\gamma\bar{F}| \ll 1$.[27]

In this paper, we propose a modulated pre- and post-selected measurement (PPSM) scheme based on the coupling-strength-dependent modulation. With the attainable highest sensitivity and precision, the coupling strength can be further relaxed to an arbitrary magnitude. We theoretically analyze the measurement sensitivity and precision for the case of unbalanced input meter. We also give the optimal pre- and post-selected states, as well as the optimal modulation of the coupling strength that correspond to the highest precision without any approximation. Our numerical comparison demonstrates that the modulated PPSM scheme is more feasible and efficient in precisely measuring an unknown parameter.

2. Coupling-strength-dependent modulation

Consider a two-level system which is pre-selected at a state of superposition $|\psi_{\rm i}\rangle = \cos(\theta_{\rm i}/2)|0\rangle + \sin(\theta_{\rm i}/2)\,{\rm e}^{{\rm i}\phi_{\rm i}}|1\rangle$, with $|0\rangle$ and $|1\rangle$ representing the eigenstates of the observable $\hat{A} = |0\rangle\langle 0| - |1\rangle\langle 1|$. Besides, the meter is prepared at $|\Phi_{\rm i}\rangle = \int {\rm d}F\,\Phi(F)|F\rangle$, where $\Phi(F)$ represents the wave function with respect to the continuous input meter variable F. Without loss of generality, suppose that $\Phi(F)$ is the real Gaussian-shape wave function centered on $\bar{F}$ with a standard deviation ΔF, which is written as $\Phi(F) = [\pi(\Delta F)^2]^{-1/4}\exp[-(F-\bar{F})^2/2(\Delta F)^2]$. The meter then is coupled to the system with a coupling strength γ. As outlined in Section 1, in order to retain both the ultra-high measurement sensitivity and precision while extending the measurable range of the coupling strength, here we consider an additional modulation in the coupling strength, denoted as $\gamma_{\rm M}$. Therefore, the interaction Hamiltonian between the system and the meter is given as

$$\hat{H}' = (\gamma + \gamma_{\rm M})\hat{A}\otimes\hat{F}. \tag{4}$$

The system–meter joint state then is given by

$$|\Psi'\rangle = {\rm e}^{-{\rm i}\int \hat{H}'\,{\rm d}t}|\psi_{\rm i}\rangle|\Phi_{\rm i}\rangle. \tag{5}$$

In the following, we investigate the best attainable measurement precision of the coupling strength γ (i.e., the physical parameter to be measured) for the joint state $|\Psi'\rangle$. Specifically, we will introduce the Fisher information (FI) metric to represent the measurement precision of the coupling strength. FI is defined based on the maximum likelihood estimation strategy, where the lower-bound of the estimation variance (i.e., the Cramer–Rao bound) corresponds to the maximal FI.[28] In principle, more FI about the parameter to be measured contained in a joint state means that one can reach a higher measurement precision. Thus, it is worth calculating the maximal FI contained in the pure joint state $|\Psi'\rangle$, i.e., the so-called quantum fisher information (QFI)[28–30]

$$F^{\rm Q} = 4(\langle\partial_\gamma\Psi'|\partial_\gamma\Psi'\rangle - |\langle\Psi'|\partial_\gamma\Psi'\rangle|^2). \tag{6}$$

$F^{\rm Q}$ can reach its maximum $F^{\rm Q}_{\rm max} = 4\langle F^2\rangle_0 = 4\bar{F}^2 + 2\Delta F^2$ when $\cos\theta_{\rm i} = 0$, signifying the attainable best measurement precision (see Appendix A).[27] Obviously, the maximal QFI is independent of the coupling strength γ to be measured, but depends only on the initial distribution $\Phi(F)$ of the meter. As the coupling strength γ is amplified through a post-selection on the system, consider the post-selected state as $|\psi_{\rm f}\rangle = \cos(\theta_{\rm f}/2)|0\rangle + \sin(\theta_{\rm f}/2)\,{\rm e}^{{\rm i}\phi_{\rm f}}|1\rangle$. In this fashion, the meter state is described as

$$|\Phi'_{\rm f}\rangle = \frac{\langle\psi_{\rm f}|\Psi'\rangle}{\sqrt{p_{\rm d}}}, \tag{7}$$

with the successful post-selected probability $p_{\rm d} = |\langle\psi_{\rm f}|\Psi'\rangle|^2$. After the post-selection, the total intensity undergoes a large reduction while the coupling strength is significantly amplified. Now, a crucial problem arises as to whether the maximal QFI $F^{\rm Q}_{\rm max}$ contained in $|\Psi'\rangle$ can be completely retained after post-selection? Concretely, if only retaining the successfully post-selected meter state, the QFI contained in $|\Phi'_{\rm f}\rangle$ is given by

$$F_{\rm d} = p_{\rm d}Q_{\rm d}, \tag{8}$$

with $Q_{\rm d} = 4(\langle\partial_\gamma\Phi'_{\rm f}|\partial_\gamma\Phi'_{\rm f}\rangle - |\langle\Phi'_{\rm f}|\partial_\gamma\Phi'_{\rm f}\rangle|^2)$. We find that $F_{\rm d}$ has the potential to reach $F^{\rm Q}_{\rm max}$ provided that $\sin\theta_{\rm i}\sin\theta_{\rm f} = -1$. For a given $\phi = \phi_{\rm i} - \phi_{\rm f}$, the maximal $F_{\rm d}$ in the case of the unbalanced input meter (with $\bar{F} \neq 0$ and $|\bar{F}| \gg \Delta F$) corresponds to the coupling strength (see Appendix B)

$$\gamma = \frac{\phi}{2\bar{F}} - \gamma_{\rm M}. \tag{9}$$

That is to say, the highest precision (corresponding to the maximal $F_{\rm d}$) can be imparted to an arbitrary coupling strength γ by introducing an appropriate modulated quantity $\gamma_{\rm M}$. Furthermore, the maximal $F_{\rm d}$ is able to reach $F^{\rm Q}_{\rm max}$ only when $|\phi| \ll 1$. With the increase of ϕ, the maximal $F_{\rm d}$ tends to be decreased slightly (see Appendix B).

In the context of reaching the highest possible precision, the pre- and post-selected states of the system are respectively recast as

$$|\psi_{\rm i}\rangle = \frac{1}{\sqrt{2}}(|0\rangle + |1\rangle), \tag{10}$$

$$|\psi_{\rm f}\rangle = \frac{1}{\sqrt{2}}(|0\rangle\, {\rm e}^{{\rm i}\phi/2} - |1\rangle\, {\rm e}^{-{\rm i}\phi/2}), \tag{11}$$

where ϕ designates the post-selected angle of the system. Therefore, by performing the modulated PPS measurements with the coupling-strength-dependent modulation, the coupling strength γ can be extracted from the average pointer deflection in the case of unbalanced pointer, i.e.,

$$\begin{aligned}\Delta\langle F\rangle &= \frac{\int {\rm d}F F|\langle F|\Phi_{\rm f}'\rangle|^2}{p_{\rm d}} - \bar{F} \\ &= \frac{(\Delta F)^2\gamma' \exp[-(\Delta F)^2\gamma'^2]\sin(2\bar{F}\gamma' - \phi)}{1-\exp[(\Delta F)^2\gamma'^2]\cos(2\bar{F}\gamma' - \phi)} \\ &\simeq \frac{2\bar{F}\gamma' - \phi}{\gamma'},\end{aligned} \tag{12}$$

where $\gamma' = \gamma + \gamma_{\rm M}$ represents the total coupling strength. The inequality in Eq. (12) corresponds to the most precise region of the coupling strength γ to be measured. The inequality is feasible provided that $|\gamma'(\bar{F} + \Delta F)| \sim |\phi|/2$, which refers to the so-called nonlinear intermediate region.[4]

3. Comparison of standard and modulated PPSM schemes

To specifically reflect the restriction of the magnitude of the coupling strength on the measurement sensitivity and precision in the standard PPSM scheme, and the advantages of the modulated PPSM scheme, we compare the two schemes in measurement sensitivity, precision and the post-selected probability.

For the case of the unbalanced pointer, we take the time delay measurement for example, in which the frequency ω serves as the meter variable. Suppose that a Gaussian-shape wave function is centered on $\omega_0 = 2400$ THz with a standard deviation $\Delta\omega = 200$ THz. The time delay τ serves as the coupling strength to be measured. For the modulated PPS measurement, an added time delay $\tau_{\rm M}$ reconstructs a modulated interaction Hamilton $\hat{H}' = (\tau + \tau_{\rm M})\hat{A}\otimes\hat{\omega}$. Moreover, the system is considered to be a two-level system with some alternative variables, such as the polarization of the light, and the which-path of a Sagnac interferometer.

In Figs. 1(a) and 1(c), we plot the spectrum shift and the measurement sensitivity with respect to the time delay to be measured in the standard PPSM scheme, respectively. Unlike the case of balanced input meter in which the pointer shift curve is always centered at the zero-value of the coupling strength, here the spectrum shift curve depends on the post-selected angle $\phi_{\rm S}$ and is centered at the time delay $\tau = \phi_{\rm S}/2\omega_0$. In this case, the measurable range of the time delay is limited at the nonlinear intermediate region $|\tau\omega_0 - \phi_{\rm S}/2| \ll |\tau\Delta\omega|$ which shows higher sensitivity, see Fig. 1(c). As shown in Fig. 1(a), the spectrum shift curve shows a walk-off effect along the time delay induced by the increased post-selected angle. Besides, the nonlinear intermediate region tends to be broadened with the increase of the post-selected angle, resulting in the reduction of the measurement sensitivity. Overall, the standard PPSM scheme is impeded in measuring larger time delay due to the sharply decreased sensitivity.

The modulated PPSM scheme shows the superiority with the same high sensitivity retained for an arbitrary time delay, as shown in Fig. 1(d). Concretely, by adding an appropriate time-delay-dependent modulation $\tau_{\rm M}$ and keeping the small post-selected angle $\phi_{\rm M}$ unchanged, the spectrum shift curve can be centered on an arbitrary time delay $\tau = \phi_{\rm M}/2\omega_0 - \tau_{\rm M}$, see Fig. 1(c). The walk-off effect vanishes with a fixed post-selected angle. Moreover, the measurable range of the time delay is limited at the modulated nonlinear intermediate region $|\tau'\omega_0 - \phi_{\rm M}/2| \ll |\tau'\Delta\omega|$ with $\tau' = \tau + \tau_{\rm M}$.

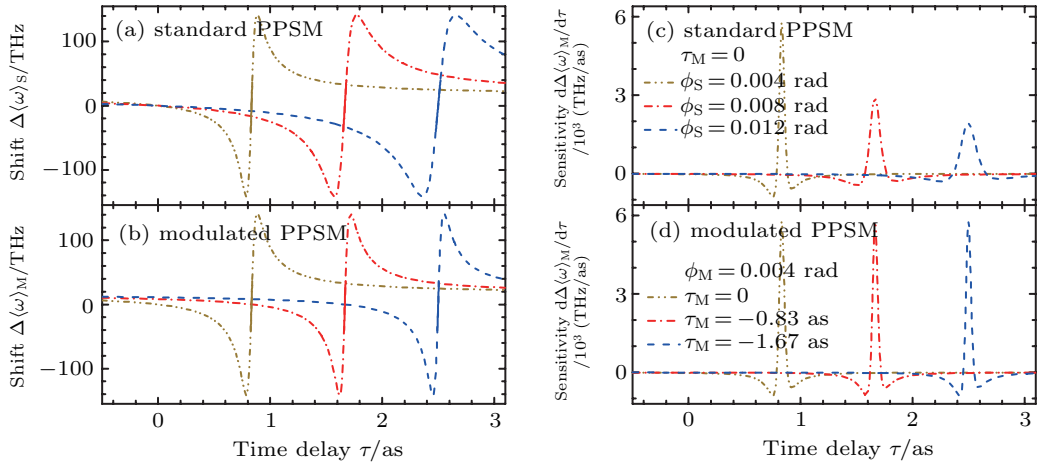


Fig. 1. Spectrum shift and measurement sensitivity with respect to time delay τ. Panels (a) and (b) show spectrum shift with respect to time delay τ in standard PPSM and modulated PPSM schemes, respectively. Panels (c) and (d) show measurement sensitivity with respect to time delay τ in standard PPSM and modulated PPSM schemes, respectively. The solid parts of the curves in panels (a) and (b) represent the corresponding nonlinear intermediate regions which are respectively limited at $|\tau\omega_0 - \phi_{\rm S}/2| \le |\tau\Delta\omega|/10$ and $|\tau'\omega_0 - \phi_{\rm M}/2| \le |\tau'\Delta\omega|/10$ for the two PPSM schemes.

As for the precision difference between the standard and the modulated PPSM schemes, we calculate the classical FI as follows:[29,31]

$$I(\tau) = p_{\rm d} \int {\rm d}\omega P(\omega|\tau)\partial_\tau^2 \ln P(\omega|\tau). \tag{13}$$

The normalized probability distribution with respect to time delay τ after a measurement on frequency is expressed as $P(\omega|\tau) = |\langle\omega|\Phi_{\rm f}'\rangle|^2$ with the post-selected probability $p_{\rm d} = \{1-\exp[-(\Delta\omega)^2\tau^2]\cos(2\omega_0\tau-\phi)\}/2$.

As can be seen in Fig. 2(a), the classical FI curve in the standard PPSM scheme reaches the maximum $I_{\max}$ at the peak time delay $\tau = \phi_{\rm S}/2\omega_0$ for a fixed post-selected angle $\phi_{\rm S}$. The peak time delay exactly falls within the nonlinear intermediate region. Unlike the measurement sensitivity as discussed above, it seems that $I_{\max}$ (approximate to $F_{\max}^{\rm Q} = 4\omega_0^2 + 2(\Delta\omega)^2$) can always be retained for different time delay with the corresponding post-selected angle. In fact, $I_{\max}$ tends to slightly reduced with the further increase of the post-selected angle (see Appendix B and Fig. B1), which is hardly shown in the most measurement scenarios. Furthermore, the classical FI at the time delay τ except for the peak time delay is increased significantly with the increase of the post-selected angle. That is to say, the measurable range of the time delay around $\tau = \phi_{\rm S}/2\omega_0$ can be increased with an increased post-selected angle from the point of view of the measurement precision.

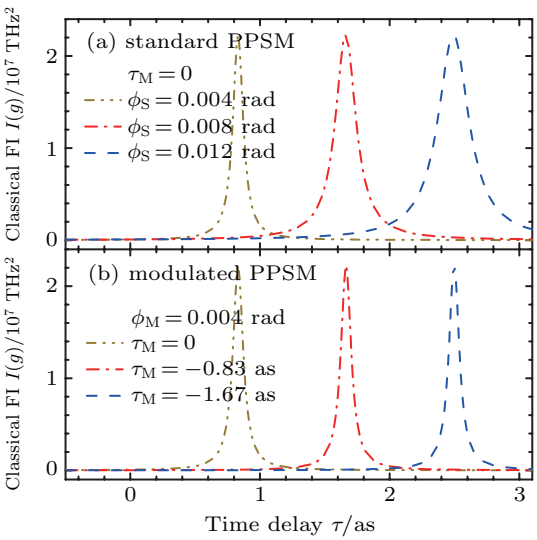


Fig. 2. Classical Fisher information as a function of the time delay τ in (a) standard PPSM scheme and (b) modulated PPSM scheme.

For contrast, it seems that in the most scenarios, the modulated PPSM scheme shows no improvement in precision, see Fig. 2(b). Combined with the sensitivity curves (see Figs. 1(c) and 1(d)), we can find that the sensitivity in PPS measurements can be improved at the sacrifice of the precision corresponding to the time delay except for the peak time delay $\tau = \phi_{\rm M}/2\omega_0 - \tau_{\rm M}$. However, it is more crucial for one to reach the attainable highest measurement sensitivity and precision. In this regard, the modulated PPSM scheme becomes the dominate scheme to reach both the highest sensitivity and precision.

In Figs. 3(a) and 3(b), we compare the post-selected probability between the standard and modulated PPSM schemes. For a fixed post-selected angle, there always exists the minimum of the post-selected probability which corresponds to the time delay τ to be measured. In the standard PPSM scheme (see Fig. 3(a)), we can see that the post-selected probability tends to be increased with the increase of the post-selected angle $\phi_{\rm S}$. More precisely, the standard PPSM scheme shows a larger post-selected probability for a larger time delay. However, in the modulated PPSM scheme, the low probability is retained for an arbitrary time delay when keeping the small post-selected angle $\phi_{\rm M}$ (corresponding to a narrow modulated intermediate region) unchanged, see Fig. 3(b).

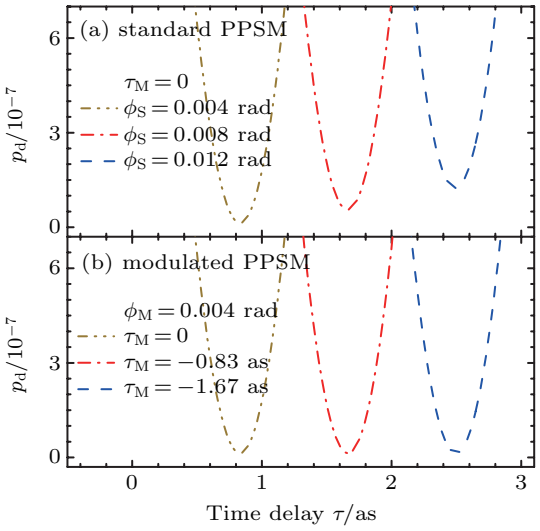


Fig. 3. Post-selected probability as a function of the time delay τ in (a) standard PPSM scheme and (b) modulated PPSM scheme.

4. Realization of the modulated PPSM scheme

The standard PPSM scheme shows extremely high sensitivity and precision for an extremely small coupling strength, but has little feasibility to attain the high sensitivity or precision with adjustable post-selection in practice. The schematic diagram of the standard PPSM scheme is shown in Fig. 4(a). For the case of the unbalanced pointer, the walk-off effect of the pointer shift curve hinders one from detecting the rough magnitude of the coupling strength to be measured. For contrast, the modulated PPSM scheme has the ability to attain both the highest sensitivity and precision for an arbitrary coupling strength. In this case, the specific strategy of performing the modulated PPSM scheme becomes much crucial.

Suppose an arbitrary coupling strength (i.e., the parameter to be measured) is expressed as $\gamma = \gamma_0 + \Delta\gamma$ with γ_0 and $\Delta\gamma$ representing the expected value of measurement out-

comes and the uncertainty, respectively. More precisely, the uncertainty $\Delta\gamma$ can be regarded as a small fluctuation of the measured coupling strength which is not detectable in general. The modulated PPSM scheme shows its significance in measuring $\Delta\gamma$ with high-precision, with a schematic diagram shown in Fig. 4(b). Concretely, the modulated PPSM scheme in the case of unbalanced pointer is performed in terms of three steps: first, the post-selected angle is chosen as $\phi_{\rm M}=\pi/4$ (which is analogous to the balanced homodyne detection[32]) and the coupling-strength-dependent modulation is set as $\gamma_{\rm M}=\phi_{\rm M}/8\bar{F}$, the coupling strength is roughly estimated as γ_0; then, the coupling-strength-dependent modulation is determined as $\gamma_{\rm M}=\phi_{\rm M}/2\bar{F}-\bar{F}$ and the post-selected angle is modulated based on $\Delta\gamma$ ($|\Delta\gamma\bar{F}-\phi_{\rm M}/2|\ll|\Delta\gamma\Delta F|$) as a function of the feedback information of the rough estimation, i.e., $\Delta\gamma$ is located within the modulated nonlinear intermediate region $|\gamma'\bar{F}-\phi_{\rm M}/2|\ll|\gamma'\Delta\omega|$; finally, the uncertainty $\Delta\gamma$ is precisely estimated.

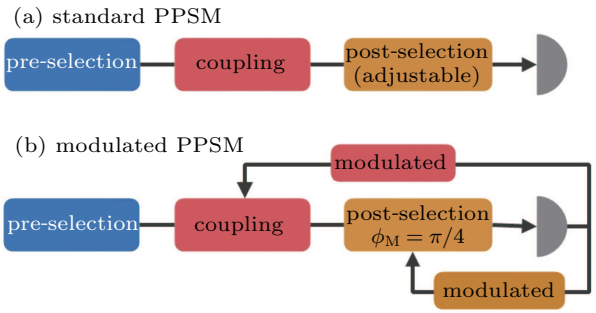


Fig. 4. Schematic diagrams of (a) standard PPSM scheme and (b) modulated PPSM scheme. In the standard PPSM scheme, the post-selection is adjustable based on the feedback outcomes. In the modulated PPSM scheme, the post-selected angle is initially set as $\phi_{\rm M}=\pi/4$; then, the coupling-strength-dependent modulation is introduced and the post-selection is modulated based on the feedback outcomes.

5. Conclusion

By including appropriate modulation in the coupling strength and the post-selection state, we are able to reach the attainable highest sensitivity and precision in the modulated PPSM scheme. We have given the optimal modulation corresponding to the optimal sensitivity and precision, which allows a precise measurement for an arbitrary coupling strength without any approximation.

In this work, we have compared the modulated PPSM scheme with the standard PPSM scheme in the case of unbalanced input meter. Both the highest sensitivity and precision may be reached only via the modulated PPSM scheme, which inevitably requires a low post-selected probability. As for the implement of the modulated PPSM scheme in practical experiments, we have given the specific strategy of performing the modulated PPSM scheme.

Appendix A: Quantum Fisher information of $|\Psi'\rangle$

Consider a two-level system pre-selected at the state $|\psi_{\rm i}\rangle=\cos(\theta_{\rm i}/2)|0\rangle+\sin(\theta_{\rm i}/2)\,{\rm e}^{{\rm i}\phi_{\rm i}}|1\rangle$, and a meter initially prepared at $|\Phi_{\rm i}\rangle=\int{\rm d}F\Phi(F)|F\rangle$ with the wave function $\Phi(F)=[\pi(\Delta F)^2]^{-1/4}\exp[-(F-\bar{F})^2/2(\Delta F)^2]$. An additional coupling-strength-dependent modulation, denoted as $\gamma_{\rm M}$, reconstructs the interaction Hamilton as $\hat{H}'=(\gamma+\gamma_{\rm M})\hat{A}\otimes\hat{F}$. The system-meter joint state then is expressed as

$$\begin{aligned}|\Psi'\rangle&={\rm e}^{-{\rm i}\int\hat{H}'{\rm d}t}|\psi_{\rm i}\rangle|\Phi_{\rm i}\rangle\\&=\int{\rm d}F\bigg[\cos\frac{\theta_{\rm i}}{2}|0\rangle\,{\rm e}^{{\rm i}(\gamma+\gamma_{\rm M})F}\\&\quad+\sin\frac{\theta_{\rm i}}{2}|1\rangle\,{\rm e}^{{\rm i}\phi_{\rm i}}\,{\rm e}^{-{\rm i}(\gamma+\gamma_{\rm M}F)}\bigg]\Phi(F)|F\rangle.\end{aligned}\tag{A1}$$

The quantum Fisher information carried by $|\Psi'\rangle$ is calculated as follows:

$$F^{\rm Q}=4(\langle\partial_\gamma\Psi'|\partial_\gamma\Psi'\rangle-|\langle\Psi'|\partial_\gamma\Psi'\rangle|^2),\tag{A2}$$

where

$$\langle\partial_\gamma\Psi'|\partial_\gamma\Psi'\rangle=\int{\rm d}FF^2\Phi^2(F)=\bar{F}^2+\frac{1}{2}(\Delta F)^2,\tag{A3}$$

$$\langle\Psi'|\partial_\gamma\Psi'\rangle={\rm i}\cos\theta_{\rm i}\int{\rm d}FF\Phi^2(F)={\rm i}\cos\theta_{\rm i}\bar{F}.\tag{A4}$$

Substituting Eqs. (A3) and (A4) into Eq. (A2), we have $F^{\rm Q}=4\bar{F}^2+2(\Delta F)^2-4\cos^2(\theta_{\rm i})\bar{F}^2$. $F^{\rm Q}$ reaches the maximum $F^{\rm Q}_{\rm max}=4\bar{F}^2+2(\Delta F)^2$ when $\cos\theta_{\rm i}=0$.

Appendix B: Quantum Fisher information of $|\Phi'_{\rm f}\rangle$

Suppose that the system is post-selected at $|\psi_{\rm f}\rangle=\cos(\theta_{\rm f}/2)|0\rangle+\sin(\theta_{\rm f}/2)\,{\rm e}^{{\rm i}\phi_{\rm f}}|1\rangle$, the normalized meter state then is written as

$$\begin{aligned}|\Phi'_{\rm f}\rangle&=\frac{\langle\psi_{\rm f}|\Psi'\rangle}{\sqrt{p_{\rm d}}}\\&=\frac{1}{\sqrt{p_{\rm d}}}\int{\rm d}F\bigg[\cos\frac{\theta_{\rm i}}{2}\cos\frac{\theta_{\rm f}}{2}\,{\rm e}^{{\rm i}(\gamma+\gamma_{\rm M})F}\\&\quad+\sin\frac{\theta_{\rm i}}{2}\sin\frac{\theta_{\rm f}}{2}\,{\rm e}^{{\rm i}\phi}\,{\rm e}^{-{\rm i}(\gamma+\gamma_{\rm M})F}\bigg]\Phi(F)|F\rangle.\end{aligned}\tag{B1}$$

Under the condition of reaching the maximal QFI of the state $|\Psi'\rangle$ (with $\cos\theta_{\rm i}=0$), the probability of successful post-selection is given by

$$p_{\rm d}=\frac{1\pm\sin\theta_{\rm f}\int{\rm d}F\cos[2(\gamma+\gamma_{\rm M})F-\phi]\Phi^2(F)}{2},\tag{B2}$$

where $\pm$ corresponds to $\sin\theta_{\rm i}=\pm1$. Hence, the normalized meter state is rewritten as

$$|\Phi'_{\rm f}\rangle=\frac{\int{\rm d}F[\cos\frac{\theta_{\rm f}}{2}\,{\rm e}^{{\rm i}(\gamma+\gamma_{\rm M})F}\pm\sin\frac{\theta_{\rm f}}{2}\,{\rm e}^{{\rm i}\phi}\,{\rm e}^{-{\rm i}(\gamma+\gamma_{\rm M})F}]\Phi(F)|F\rangle}{\sqrt{2\xi(\gamma)}},\tag{B3}$$

where we define $\xi(\gamma)=\sqrt{p_{\rm d}}$ for later analysis. Then, we have

$$|\partial_\gamma\Phi_{\rm f}'\rangle=\frac{1}{\sqrt{2}\xi^2(F)}\int {\rm d}F\Big\{\cos\frac{\theta_{\rm f}}{2}{\rm e}^{{\rm i}\gamma' F}[{\rm i}F\xi(\gamma)-\xi'(\gamma)] \pm\sin\frac{\theta_{\rm f}}{2}{\rm e}^{{\rm i}\phi}{\rm e}^{-{\rm i}\gamma' F}[-{\rm i}F\xi(\gamma)-\xi'(\gamma)]\Big\}\Phi(F)|F\rangle, \tag{B4}$$

$$\langle\partial_\gamma\Phi_{\rm f}'|\partial_\gamma\Phi_{\rm f}'\rangle=\frac{1}{2\xi^4(\gamma)}\int {\rm d}F\{F^2\xi^2(\gamma)+\xi'^2(\gamma) \pm[-F^2\xi^2(\gamma)+\xi'^2(\gamma)]\sin\theta_{\rm f}\cos(2\gamma' F-\phi) \pm F\xi(\gamma)\xi'(\gamma)\sin\theta_{\rm f}\sin(2\gamma' F-\phi)\}\Phi^2(F), \tag{B5}$$

$$\langle\Phi_{\rm f}'|\partial_\gamma\Phi_{\rm f}'\rangle=\frac{1}{2\xi^3(\gamma)}\int {\rm d}F\{{\rm i}F\xi(\gamma)\cos\theta_{\rm f}-\xi'(\gamma) \mp\sin\theta_{\rm f}[F\xi(\gamma)\sin(2\gamma' F-\phi) +\xi'(\gamma)\cos(\gamma' F-\phi)]\}\Phi^2(F), \tag{B6}$$

where $\gamma'=\gamma+\gamma_{\rm M}$ denotes the total coupling strength.

For the case of unbalanced pointer (with $\bar{F}\neq 0$ and $|\bar{F}|\gg\Delta F$), the QFI of the state $\Phi_{\rm f}'$ is calculated as

$$\begin{aligned}F_{\rm d}&=4p_{\rm d}(\langle\partial_\gamma\Phi_{\rm f}'|\partial_\gamma\Phi_{\rm f}'\rangle-|\langle\Phi_{\rm f}'|\partial_\gamma\Phi_{\rm f}'\rangle|^2)\\&\simeq[2\bar{F}^2+(\Delta F)^2](1+\eta)-2\eta\gamma'^2(\Delta F)^4\\&\quad+2(1-\eta)\zeta'^2(\gamma)/\zeta^2(\gamma)-2\eta\gamma'(\Delta F)^2\zeta'(\gamma)/\zeta(\gamma)\\&\quad-[1-\eta\gamma'(\Delta F)^2-\eta]^2\zeta'^2(\gamma)/\zeta^4(\gamma)\\&\simeq 4\bar{F}^2+2(\Delta F)^2,\end{aligned} \tag{B7}$$

where $\eta=\exp[-\gamma'^2(\Delta F)^2]$. The first approximation is feasible with $\phi=2(\gamma+\gamma_{\rm M})\bar{F}$, $\zeta(\gamma)$ and $\zeta'(\gamma)$ denote the corresponding $\xi(\gamma)$ and $\xi'(\gamma)$ under this approximation, respectively. The second approximation is feasible with $|(\gamma+\gamma_{\rm M})\Delta F|\ll 1$. Obviously, the maximal QFI $F_{\rm max}^{\rm Q}=4\bar{F}^2+2(\Delta F)^2$ of the state $|\Psi'\rangle$ can be completely retained under these approximations. Note that these approximations are derived provided that $\sin\theta_{\rm i}\sin\theta_{\rm f}=-1$. Figure B1 shows the influence of the total coupling strength $\gamma'=\gamma+\gamma_{\rm M}$ on the QFI of the state $|\Phi_{\rm f}'\rangle$ under the condition that $\phi=2(\gamma+\gamma_{\rm M})\bar{F}$, which is exampled by the time delay measurements (with τ' serving as γ') discussed in the main text. We can see that $F_{\rm d}$ undergoes only a slight reduction for a large range of the time delay τ'. In the modulated PPSM scheme, by introducing an appropriate modulation $\tau_{\rm M}$ to meet $|\tau'\Delta\omega|\ll 1$, the maximal FI $F_{\rm max}^{\rm Q}$ can always be retained for an arbitrary time delay τ to be measured. In analogy to the standard PPSM scheme ($\tau_{\rm M}=0$), $F_{\rm d}$ tends to be slightly reduced with the increase of the time delay τ to be measured. For the case of the unbalanced pointer, this reduction of QFI is hardly shown in the most measurement scenarios.

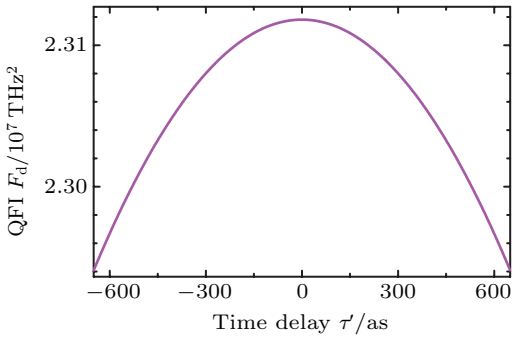


Fig. B1. Quantum Fisher information of the state $|\Phi_{\rm f}'\rangle$ as a function of the total time delay $\tau'=\tau+\tau_{\rm M}$ under the condition $\phi_{\rm M}=2(\tau+\tau_{\rm M})\omega_0$.

References

[1] Aharonov Y, Bergmann P G and Lebowitz J L 1964 *Phys. Rev. B* **134** 1410
[2] Aharonov Y, Albert D Z and Vaidman L 1988 *Phys. Rev. Lett.* **60** 1351
[3] Zhu X, Zhang Y, Pang S, Qiao C, Liu Q and Wu S 2011 *Phys. Rev. A* **84** 052111
[4] Kofman A G, Ashhab S and Nori F 2012 *Phys. Rep.* **520** 43
[5] Hosten O and Kwiat P 2008 *Science* **319** 787
[6] Kocsis S, Braverman B, Ravets S, Stevens M J, Mirin R P, Shalm L K and Steinberg A M 2010 *Science* **332** 1170
[7] Starling D J, Dixon P B, Jordan A N and Howell J C 2010 *Phys. Rev. A* **82** 063822
[8] Zhou X, Ling X, Luo H and Wen S 2012 *Appl. Phys. Lett.* **101** 251602
[9] Xu X Y, Kedem Y, Sun K, Vaidman L, Li C F and Guo G C 2013 *Phys. Rev. Lett.* **111** 033604
[10] Salazar-Serrano L J, Janner D, Brunner N, Pruneri V and Torres J P 2014 *Phys. Rev. A* **89** 012126
[11] Magaña-Loaiza O S, Mirhosseini M, Rodenburg B and Boyd R W 2014 *Phys. Rev. Lett.* **112** 200401
[12] Qiu X, Zhou X, Hu D, Du J, Gao F, Zhang Z and Luo H 2014 *Appl. Phys. Lett.* **105** 131111
[13] Rhee H, Eom I, Ahn S H, Song K H and Cho M 2015 *Phys. Rev. A* **91** 053839
[14] Qiu J, Ren C and Zhang Z 2016 *Phys. Rev. A* **93** 063841
[15] Zhang Y, Li D, He Y, Shen Z and He Q 2016 *Opt. Lett.* **41** 5409
[16] Luo L, Qiu X, Xie L, Liu X, Li Z, Zhang Z and Du J 2017 *Opt. Express* **25** 21107
[17] Xie L, Qiu X, Luo L, Liu X, Li Z, Zhang Z, Du J and Wang D 2017 *Appl. Phys. Lett.* **111** 191106
[18] Li L, Li Y, Zhang Y L, Yu S, Lu C Y, Liu N L, Zhang J and Pan J W 2018 *Phys. Rev. A* **97** 033851
[19] Huang J Z, Fang C and Zeng G 2018 *Phys. Rev. A* **97** 063853
[20] Yakir A, Sandu P and Jeff T 2010 *Phys. Today* **63** 27
[21] Duck I M, Stevenson P M and Sudarshan E C G 1989 *Phys. Rev. D* **40** 2112
[22] Jozsa R 2007 *Phys. Rev. A* **76** 044103
[23] Tollaksen J, Aharonov Y, Casher A, Kaufherr T and Nussinov S 2010 *New J. Phys.* **12** 013023
[24] Dixon P B, Starling D J, Jordan A N and Howell J C 2009 *Phys. Rev. Lett.* **102** 173601
[25] Brunner N and Simon C 2010 *Phys. Rev. Lett.* **105** 010405
[26] Zhang Z H, Chen G, Xu X Y, Tang J S, Zhang W H, Han Y J, Li C F and Guo G C 2016 *Phys. Rev. A* **94** 053843
[27] Li F, Huang J and Zeng G 2017 *Phys. Rev. A* **96** 032112
[28] Braunstein S L and Caves C M 1994 *Phys. Rev. Lett.* **72** 3439
[29] Braunstein S L, Caves C M and Milburn G J 1996 *Ann. Phys.* **247** 135
[30] Pang S and Brun T A 2015 *Phys. Rev. Lett.* **115** 120401
[31] Fisher R A 1925 *Math. Proc. Cambridge Philos. Soc.* **22** 700
[32] Qiu X, Xie L, Liu X, Luo L, Li Z, Zhang Z and Du J 2017 *Appl. Phys. Lett.* **110** 071105